Comparison of multifrequency acoustic and *in situ* measurements of zooplankton abundances in Knight Inlet, British Columbia

Mark V. Trevorrow[a)]
Defence Research and Development Canada—Atlantic, PO Box 1012, Dartmouth, Nova Scotia, B2Y 3Z7, Canada

David L. Mackas
Institute of Ocean Sciences, 9860 W. Saanich Road, Sidney, British Columbia, V8L 4B2, Canada

Mark C. Benfield
Department of Oceanography and Coastal Sciences, Louisiana State University, Wetland Resources, Baton Rouge, Louisiana 70803

(Received 18 June 2004; revised 28 February 2005; accepted 29 March 2005)

An investigation of midwater zooplankton aggregations in a coastal fjord was conducted in November 2002. This study focused on quantitative comparisons between a calibrated, three-frequency (38, 120, and 200 kHz) vessel-based echo-sounder, a multinet towed zooplankton sampler (BIONESS), and a high-resolution underwater camera (ZOOVIS). Daytime layers of euphausiids and amphipods near 70–90-m depth were observed in lower parts of the inlet, especially concentrated by tidal flows around a sill. Quantitative backscatter measurements of euphausiids and amphipods, combined with *in situ* size and abundance estimates, and using an assumed tilt-angle distribution, were in agreement with averaged fluid-cylinder scattering models produced by Stanton and Chu [ICES J. Mar. Sci. **57**, 793–807, (2000)]. Acoustic measurements of physonect siphonophores in the upper inlet were found to have a strong 38-kHz scattering strength, in agreement with a damped bubble scattering model using a diameter of 0.4 mm. In relatively dense euphausiid layers, ZOOVIS abundance estimates were found to be a factor of 2 to 4 higher than the acoustic estimates, potentially due to deviations from assumed euphausiid orientation. Nocturnal near-surface euphausiid scattering exhibited a strong (15 dB) and rapid (seconds) sensitivity to vessel lights, interpreted as due to changing animal orientation. [DOI: 10.1121/1.1920087]

PACS numbers: 43.30.Sf, 43.30.Ft [KGF] Pages: 3574–3588

I. INTRODUCTION

High-frequency echo-sounders can be useful for assessing abundance and spatial distributions of meso-zooplankton such as crustaceans, pteropods, and siphonophores. Typical zooplankton echo-sounders, operating at frequencies in excess of 30 kHz, offer high spatial-temporal resolution and useful sensitivity to depths up to 200 m. When vessel mounted, these sounders can perform rapid surveys of zooplankton scattering layers, and are particularly useful for assessing small-scale patchiness and vertical layering. The drawbacks of purely acoustic surveys are an uncertain knowledge of the scatterer type (i.e., species and size), combined with an uncertainty regarding appropriate acoustic scattering models, making it difficult to estimate the absolute abundance using acoustics alone. When combined with net trawls and/or new *in situ* optical tools, however, accurate surveys of zooplankton abundances are feasible (Wiebe *et al.*, 1997; Greene *et al.*, 1998). These *in situ* samples provide the necessary data on the species, sizes, orientation, and abundances at specific depths or locations. The link between acoustic and *in situ* sampling approaches is a reliable acoustic scattering model for a particular zooplankton type. Of course, *in situ* sampling is more difficult, the postanalysis of net samples is time-consuming, and both nets and optical techniques lack the *volumetric coverage rate* of the echo-sounders. Therefore, the thrust of this work is to demonstrate a combined acoustic vs *in situ* measurement approach, including a validation of generic scattering models for two zooplankton types.

Quantitatively, the acoustic backscatter strength is related to the zooplankter type, orientation, and their abundance within the insonified volume. It is well known that a *single*-frequency echo-sounder cannot generally distinguish between mixtures of different zooplankton sizes or species (e.g., Greene *et al.*, 1989; Holliday and Pieper, 1993). Similarly, it has been found that single-frequency systems have difficulties distinguishing between zooplankton and colocated turbulent microstructure scattering (Stanton *et al.*, 1994; Trevorrow, 1998). Thus, single-frequency systems are only useful in nonturbulent regions dominated by a single species, or in situations where different species can be distinguished on the basis of behavior (e.g., depth). Such situations were found in this study. A more general approach is the simultaneous use of multiple acoustic frequencies, typically 30 to 1000 kHz, as demonstrated in several previous

[a)]Electronic mail: mark.trevorrow@drdc-rddc.gc.ca

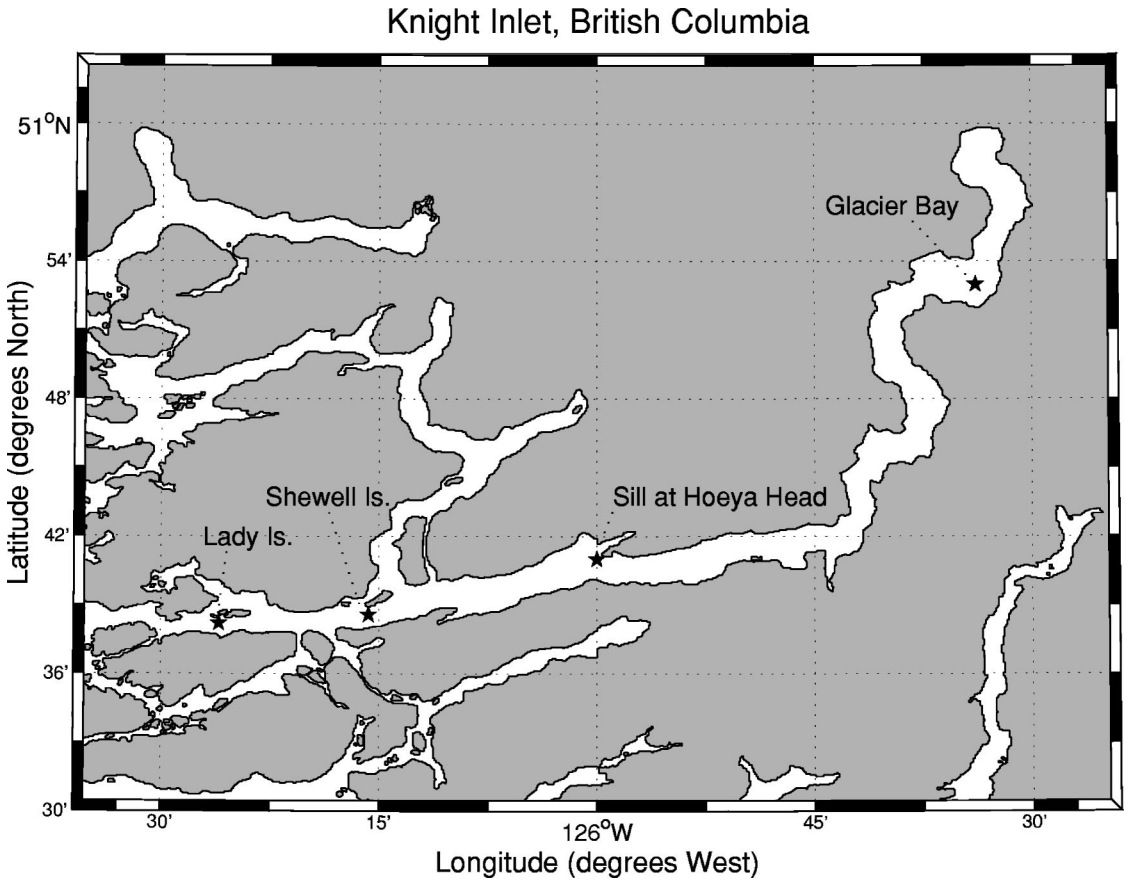

FIG. 1. Map of Knight Inlet showing locations of data collection sites.

studies (e.g., Greenlaw, 1979; Holliday and Pieper, 1980; Greene *et al.*, 1989; Trevorrow and Tanaka, 1995; Wiebe *et al.*, 1997). Because the scattering functions for crustacean zooplankton are strongly size-and frequency dependent, variations in scattering strength with frequency can be used to infer animal sizes. Without *in situ* data on zooplankton species and sizes, however, appropriate scattering models cannot be chosen with certainty.

This study combined a three-frequency, vessel-based echo-sounder system with BIONESS multinet plankton trawls and a newly developed *in situ* optical imaging system known as ZOOVIS. The surveys were performed at various locations in Knight Inlet, British Columbia (B.C.) as part of an investigation on mechanism for zooplankton aggregation at coastal sills. Two separate 15-day sea trials were conducted in November 2001 and 2002. Knight Inlet has been the site of several recent oceanographic experiments (e.g., Farmer and Armi, 1999a, b; Klymak and Gregg, 2001, 2003, 2004) focused on internal hydraulics, and turns out to be a unique natural laboratory for study of zooplankton abundance and aggregation. This work will demonstrate several examples where the combination of acoustic versus *in situ* samples can be used to verify generic zooplankton scattering models.

II. EXPERIMENTAL DESCRIPTION

A. Overview of the physical and ecological setting

Knight Inlet is a fjord located on the south-central coast of British Columbia, fed by a glacier at its head some 90 km inland, and open to the coastal Pacific through Queen Charlotte Sound at its mouth. Knight Inlet is relatively calm, with comparatively light winds and largely sheltered from oceanic wave action, making it ideal for survey operations. The lower part of Knight Inlet trends approximately WSW and has a roughly uniform width (see Fig. 1), whereas the upper half of the Inlet trends more north–south. The inlet is quite steep-sided, with side-wall slopes near 45° and mountain peaks on each side reaching over 1000 m above sea level. In the middle of the lower section there is an underwater sill running approximately north–south, roughly perpendicular to the east–west tidal flow, with typical crest depth near 65 m. This sill region has been the focus of extensive internal hydraulics investigations (Farmer and Armi, 1999a, b; Klymak ans Gregg, 2001, 2003, 2004; Ross and Lueck, 2003). To the west of the sill the seabed falls away to a flat bottom roughly 150 m deep, while on the eastern side and in the upper inlet there is a deeper basin with depths more than 500 m.

The area has dominantly semidiurnal tides, with a strong fortnightly modulation and tidal heights ranging from 1.0 to 4.5 m. The flood tide runs eastward and northward. Typical peak tidal currents over the sill are near $1.5\,\mathrm{m\,s^{-1}}$. During the late autumn Knight Inlet features a strong near-surface stratification, with a colder, fresher (7.5 °C, 26-psu) surface layer from 6–10-m deep with relatively well-mixed conditions (8.0 °C, 32 psu) in the deeper waters. Vertical gradients of temperature, salinity, and density within the 2–5-m thick pycnocline were typically strong (maxima approximately

$0.06\,^{\circ}\mathrm{C\,m^{-1}}$, $1.6\,\mathrm{psu\,m^{-1}}$, and $1.8\,\mathrm{kg\,m^{-4}}$). The deep waters (>50 m) in the eastern basin and upper inlet tend to be slightly fresher than on the west side of the sill.

Ecologically, Knight Inlet is similar to other B.C. coastal inlets. In these inlets zooplankton scattering layers are commonly observed at 60–90-m depth in the daytime, exhibiting clear nocturnal migration to the near surface. These layers are generally composed of larger crustacean zooplankton such as euphausiids (dominated by *E. pacifica*), amphipods (both hyperiid and gammarid), copepods, and various shrimp (Mackie and Mills, 1983). Other species of pteropods, chaetognaths, ctenophores, and cnidaria are sometimes present, and known to migrate diurnally from the surface through depths of 250 m. However, in the context of interpreting echo-sounding data these other species can be largely ignored due to the combination of their low abundance and small target strength (these are soft-bodied animals). The exception to this is the hard-shelled planktonic pteropod *Limacina helicina*, which for typical animal size near 3 mm have a target strength at 200 kHz near -76 dB (Stanton *et al.*, 1998), similar to that of adult euphausiids. A few *L. helicina* were collected in the BIONESS trawls, with abundance ranging from zero to a maximum of $6.8\,\mathrm{per\,m^3}$. All examples discussed in this work had negligible abundances of *L. helicina*.

The most numerically abundant zooplankton type in the inlet are copepods, with adults reaching up to 4 mm in length. *Neocalanus plumchrus* appears to be the most common species in B.C. coastal waters (Harrison *et al.*, 1983). *Neocalanus spp.* generally do not migrate on a daily basis, and in the midsummer the adults dive to deep waters to overwinter (diapause) and thus were not present in these November surveys. Other smaller copepod species (*Calanus marshallae, C. pacificus, Pseudocalanus spp.*, and *Metridia pacifica*) are common in B.C. coastal waters, including Knight Inlet, and these generally exhibit similar seasonal migration. Owing to the combination of the small size of the adult copepods relative to the euphausiids and amphipods, and their relatively low abundances in the scattering layers ($\mathrm{typically} < 100\,\mathrm{per\,m^3}$), scattering from copepod species is ignored in this work.

In contrast to the crustacean scattering dominant in the lower inlet, acoustic scattering signatures in the upper inlet appeared to be dominated by the physonect siphonophores. This type of siphonophore is a relatively strong acoustic scatterer due to the presence of a small gas-filled bubble (the pneumatophore) at the top of the colony. Unfortunately, trawl nets usually destroy these delicate siphonophore colonies, such that abundances can only be inferred from counting remaining component parts (e.g., nectophores). Using visual observations from a submersible, Mackie (1985) reported significant abundances of *Nanomia cara* in Knight Inlet and other B.C. coastal inlets.

B. Instrumentation and methods

The primary acoustic tool used during the Nov. 2002 surveys was a three-frequency (38, 120, and 200 kHz) echo-sounder system mounted on the *CCGS* VECTOR. This system was utilized to both map out the spatial distributions of meso-zooplankton, and for detailed comparison with the BIONESS and ZOOVIS. The 120-kHz sounder proved to be the most useful in this study, as it was sensitive to both fish and zooplankton aggregations and the backscatter from turbulent microstructure that is a feature of the internal flow regime near the sill.

During the Nov. 2002 surveys the single-beam three echo-sounder transducers were mounted in a single fairing at a depth of 3.5 m approximately 25 m forward of the stern. The transducers were oriented vertically downward. The beamwidths of the transducers were approximately matched, being 9.5°, 9.0°, and 7.0° (total width to -3 dB) for the 38-, 120-, and 200-kHz transducers respectively, so that the overall insonified volumes were similar. Transducer beam patterns were provided by the manufacturer. The echo-sounder transmitter–receiver electronics were custom built at the Institute of Ocean Sciences (Sidney, B.C.), with echo-sounder control, data acquisition, and display performed by an accompanying PC. During all survey runs the echo-sounder was operated at a 1.0-Hz ping rate, with all channels simultaneously transmitting a 0.5-ms (37-cm acoustic resolution) gated-cw pulse. The acoustic source levels for all three transducers were near 221 dB ($re:\mu$Pa at 1 m). At this source level acoustic cavitation effects were not considered to be a problem due to the relatively high acoustic frequencies, short pulse length, and very low duty cycle (see Medwin and Clay, 1998). Echo intensity from each channel was sampled at 12 500 samples per second (6-cm sampling resolution) with 16-bit (93-dB) dynamic range. The nominal maximum recording depth was 200 m. In addition to the acoustic data, time and DGPS position were recorded for each ping. During echo-sounder surveys the ship maintained a speed of roughly 6 knots ($3\,\mathrm{m\,s^{-1}}$) relative to the ground, except during BIONESS trawls where the speed was reduced to roughly 3 knots and during ZOOVIS deployments where the speed was 1 to 2 knots.

Sea-truth samples of zooplankton abundance, size, and species composition were obtained by towing a BIONESS (Bedford Institute of Oceanography Net and Environmental Sampling System) instrumented multiple net sampler (Sameoto *et al.*, 1980) at selected locations. The BIONESS carried nine nets that were opened in sequence. Each net had a mouth area of $0.25\,\mathrm{m^2}$ and a mesh size of 0.23 mm. Depth and cumulative volume filtered were continuously monitored with a pressure sensor and flow-meter interfaced to a Seabird Electronics CTD mounted on the BIONESS. The BIONESS was either towed horizontally or obliquely at a forward speed of about $1.5\,\mathrm{m\,s^{-1}}$. The nets were opened and closed in sequence, either to divide the water column into a stacked series of depth strata, or to obtain a horizontal sequence of samples from one depth stratum (e.g., tracking an euphausiid scattering layer). The echo-sounders were used during the BIONESS tows to guide the nets to particular zooplankton scattering layers, and to prevent impact with the seabed. The entire sample from each BIONESS tow stratum was preserved in 10% formalin and returned to the laboratory for identification and enumeration. The entire sample was examined for abundance and body size of large and/or rare taxa

(e.g., euphausiids, amphipods, gelatinous zooplankton). The sample was then quantitatively subsampled using a Folsom splitter for counts of small abundant taxa (e.g., copepods). Total counting effort was sufficient to give an expected subsampling error of roughly 5%–10% for the dominant species.

The Zooplankton Visualization and Imaging System (ZOOVIS) is a high-resolution digital camera system designed to collect quantitative data on the numbers, sizes, and identities of meso-and macro-zooplankton at depths up to 250 m. A detailed description of this system can be found in Benfield *et al.* (2003a). ZOOVIS was capable of resolving anatomical details of organisms larger than 1–2 mm in size within a sampling volume approximately 40 cm away from the camera. Sampling volumes ranged from 0.36 to 3.4 liters depending on camera settings. Images were acquired at 4–8-s intervals while the instrument was profiled up and down at $50\,\mathrm{cm\,s^{-1}}$ with the vessel steaming at 1–2 knots. Similarly to BIONESS, real-time echo-sounder images were used to guide ZOOVIS to particular scattering layers. Due to shipboard logistical constraints, however, ZOOVIS and BIONESS could not be deployed simultaneously. Images were analyzed through a combination of visual inspection and postprocessed with an image processor that located and measured targets. Euphausiid sizes were estimated by measuring their widths and converting to length using an allometric relationship determined from preserved *Euphausia pacifica* collected on 19 Nov. 2002. Euphausiid abundances were estimated by summing all detected euphausiids and dividing by the corresponding imaging volume.

C. Acoustic postprocessing

For quantitative purposes, the raw echo-sounder amplitude vs range data, $A(r)$, must be converted to volumetric backscatter strength, S_v, defined as the decibel equivalent of the backscatter cross section per unit volume (units of dB $re:\mathrm{m}^{-1}$). This conversion is accomplished through the standard sonar equation (e.g., Medwin and Clay, 1998), i.e.,

$$S_v(r) = 20\log_{10}[A(r)] + K + 40\log_{10}[r] + 2\cdot\alpha\cdot r - 10\log_{10}[U(r)] - \mathrm{TVG}(r), \quad (1)$$

where K is the calibration coefficient, r is downward range, α is the acoustic absorption, $U(r)$ is the insonified volume, and TVG is the preamplifier time-varying gain. The calibration coefficient K includes transmit power level, transducer sensitivity, fixed amplifier gain, and A/D conversion factors. The echo-sounder TVG approximated a $20\cdot\log_{10}[r]$ function within the 60 ms after transmission and was held constant at greater depths. The TVG was measured for each channel by averaging echo-data with the transmitter turned off, then normalizing such that TVG at $r=1$ m was zero. The TVG was not changed during these field trials. The acoustic absorption is frequency- and environment dependent, and for the typical (depth-averaged) water conditions in Knight Inlet has a values of 0.0093, 0.033, and $0.047\,\mathrm{dB\,m^{-1}}$ at 38, 120, and 200 kHz, respectively (Francois and Garrison, 1982). In terms of the *equivalent solid angle* of the transducer, φ, and the pulse duration, $\tau(=500\ \mu\mathrm{s})$, the insonified volume is given by

$$U(r) = \frac{1}{3}\varphi\left[\left(r+\frac{1}{4}c\tau\right)^3 - \left(r-\frac{1}{4}c\tau\right)^3\right]. \quad (2)$$

For the sounders used in Knight Inlet the insonified volume increased from roughly $0.5\ \mathrm{m}^3$ at 10-m range to $30-50\ \mathrm{m}^3$ at 80 m (the nominal zooplankton layer depth). Within the zooplankton layers these sampling volumes are comparable to that sampled with the BIONESS, but much larger than sampled per image by ZOOVIS.

The three echo-sounders were acoustically calibrated using the backscatter from precisely machined tungsten-carbide spheres (38-, 40-, and 42.9-mm diameter) suspended along the center line of the acoustic beams (following methods outlined in Vagle *et al.*, 1996). Multiple calibration trials were conducted while the ship was anchored at night. The calibrations were estimated to be accurate to ± 0.8 dB, or a relative error of 20% in cross section. The greatest source of error in this was uncertainty in alignment of the target spheres on the transducer axes. The calibration data were carefully selected by moving the sphere through the transducer beams until maxima were found; however, some instabilities in echo amplitude attributable to target sphere movement were observed. Clearly, more accurate calibrations can be obtained using split-beam sounders which can measure the target location relative to the beam.

The electronic noise levels of the echo-sounder electronics created some limitations for zooplankton sampling, especially for the 200-kHz channel at greater depths. Because of the range variations in Eq. (1), these noise levels were also range dependent. Specific systemic noise curves were measured for each channel by recording and averaging echo data with the transmitters turned off. These noise curves are included in all following plots of S_v vs depth to show the measurement signal-to-noise ratio. In all quantitative S_v calculations, usually involving averaging in depth and ping, these noise levels were used to correct for noise contamination, as described in Korneliussen (2000) and Watkins and Brierley (1996). The correction was applied by simply subtracting the equivalent volume backscatter cross section of the noise from the volume scattering cross-section data on a ping-by-ping basis. For moderate to high signal-to-noise data this correction to the averaged S_v is small (<0.5 dB); however, corrections up to 2.5 dB were found in 200-kHz data near the bottom of some scattering layers. An additional signal conditioning process was applied to remove contamination from occasional, large targets (identity unknown) embedded in the zooplankton layers. During ping averaging through zooplankton scattering layers, echoes exceeding an upper S_v threshold in each channel were removed. These upper thresholds were set 10 dB above the maximum layer-averaged S_v in each channel, typically -80 to -70 dB depending on the situation. This contamination was most apparent in crustacean scattering in the 38-kHz channel, where the expected S_v were <-90 dB.

III. CRUSTACEAN AND SIPHONOPHORE SCATTERING MODELS

To proceed from acoustic backscatter strength to *in situ* abundance estimates, several basic facts need to be estab-

lished. The local species and size composition needs to be determined (usually with a net sample), and this species and size composition is assumed to be constant throughout a local survey region. For the purposes of verifying scattering models it is preferable that the acoustic scattering be dominated by a particular species or scatterer type. If the scattering is due to multispecies ensembles, then the composition ratios between major constituents should be reasonably well known. In the case of Knight Inlet, the BIONESS trawls showed that the acoustic scattering in the lower inlet were generally dominated by euphausiids with length near 16 mm, as they are larger and generally in greater abundance than other species. Other zooplankters, such as amphipods, adult copepods, pteropods, and siphonophores, were sometimes found in moderate quantities, and at low euphausiid abundances they sometimes gave significant contributions to the acoustic backscatter. In the upper Inlet (Glacier Bay), the backscattering was dominated by physonect siphonophores, and the net trawls found negligible quantities of euphausiids and amphipods. Three distinct cases will be examined separately in Sec. IV.

Following from the assumption of a particular scatterer type, an accurate model for the acoustic scattering strength as a function of acoustic frequency and zooplankter size must be found. For euphausiids and amphipods, a number of simple models have been proposed (e.g., Johnson, 1977; Stanton, 1989), but the most appropriate in this situation is a size- and orientation-averaged fluid cylinder model recommended by Stanton and Chu (2000), based on earlier models by Stanton *et al.* (1993). This model is appropriate due to the moderately large insonified volumes of these echo-sounders (typically near $30-50\ \mathrm{m}^3$ at the euphausiid layer depth of 60–80 m), such that the echo has contributions from potentially hundreds of animals. Furthermore, the detailed acoustic scattering models generally show a strong sensitivity to zooplankter orientation (i.e., swimming angle with respect to horizontal, i.e., angle = zero implies dorsal incidence), and generally it should be expected that a natural population would have some distribution of this orientation angle about a mean value.

The specific model used here assumes the euphausiids or amphipods to be bent fluid cylinders with radius of curvature $3\times$ body length, a specific length-to-radius ratio, a Gaussian-distributed length (i.e., characterized by a mean and standard deviation), and a Gaussian-distributed orientation angle, again quantified by a mean and standard deviation. The sound-speed and density contrasts in this fluid model were assumed to be 1.03 and 1.04, respectively, following recommendations in Foote *et al.* (1990). Given all these assumptions in combination with net trawl data, the averaged backscatter cross section (σ_b, units of m^2) per animal can be calculated using the modeling equations outlined in Stanton and Chu (2000). One limitation in this formulation is the requirement that the orientation distribution include lateral (dorsal) incidence. The data on euphausiid and amphipod length and aspect ratio come from BIONESS trawl data collected near the sill and at several sites in the western inlet. Also, Stanton *et al.* (1993) showed that this averaged model is insensitive to the amount of curvature, so only a nominal value is assumed. We shall follow the notation suggested by Stanton and Chu where N (mean, std. dev.) specifies the distribution of zooplankter orientation angle (assumed Gaussian, zero = horizontal). A limiting case of orientation angle, denoted *uniformly distributed*, occurs where there is no preferred orientation and averaging occurs over all possible orientations from 0° to 360°. Based on results from Chu *et al.* (1993), the swimming angle distribution was kept as a free parameter to allow some inference of orientation from a best fit to abundances from the BIONESS trawls. Ideally, a full verification of the model could be accomplished through inclusion of *in situ* animal orientations from ZOOVIS. Unfortunately, in most cases examined in this work insufficient numbers of animals were sampled by ZOOVIS to establish reliable swimming angle distributions.

The backscatter from physonect siphonophores is dramatically different from the crustacean model discussed above. The presence of the gas-filled pneumatophore yields a much higher scattering strength than equivalent fluid models, and the radial oscillations of the approximately spherical bubble give rise to a resonant peak. One feature of siphonophores is their apparent ability to maintain a constant pneumatophore volume over a large range of depths, thereby maintaining a constant buoyancy (Benfield *et al.*, 2003b). As a first approximation, the backscatter from the pneumatophore can be modeled as a bubble (Stanton *et al.*, 1998; Warren *et al.*, 2001; Benfield *et al.* 2003b), for which there are well-established models. The backscatter from other fluid-like tissue in the siphonophore colony is significantly weaker than the bubble scatter and can be ignored. This work will follow the textbook formulation for bubble scattering as outlined in Medwin and Clay (1998), whereby the backscatter cross section for a bubble of radius, a, is given by

$$\sigma_b(f,z)=\frac{a^2}{[(f_R/f)^2-1]^2+\delta^2}, \tag{3}$$

where δ is the bubble total damping coefficient, and the bubble resonance frequency is given by

$$f_R=(2\pi a)^{-1}\sqrt{3\gamma P_0/\rho_w}, \tag{4}$$

where P_0 is the static pressure (Pa) on the bubble ($1.013\times10^5+\rho_w\cdot g\cdot z$), γ is the ratio of specific heats at constant pressure and volume of the enclosed gas ($=1.4$ for air), and ρ_w is the density ($\mathrm{kg\,m}^{-3}$) of the surrounding water. For example, a 1-mm-diameter bubble at 50-m depth has a resonant frequency of 15.8 kHz. Note that the total damping coefficient is the sum of three separate terms, i.e., damping due to reradiation, fluid viscosity, and surface tension (see Medwin and Clay, 1998 for specific evaluation of these terms for natural bubbles). It is speculated that the tissue surrounding the bubble in the pneumatophore will exhibit stronger viscous and surface tension damping than for an ordinary bubble in seawater, and the *in situ* scattering data examined here allow some exploration of this idea.

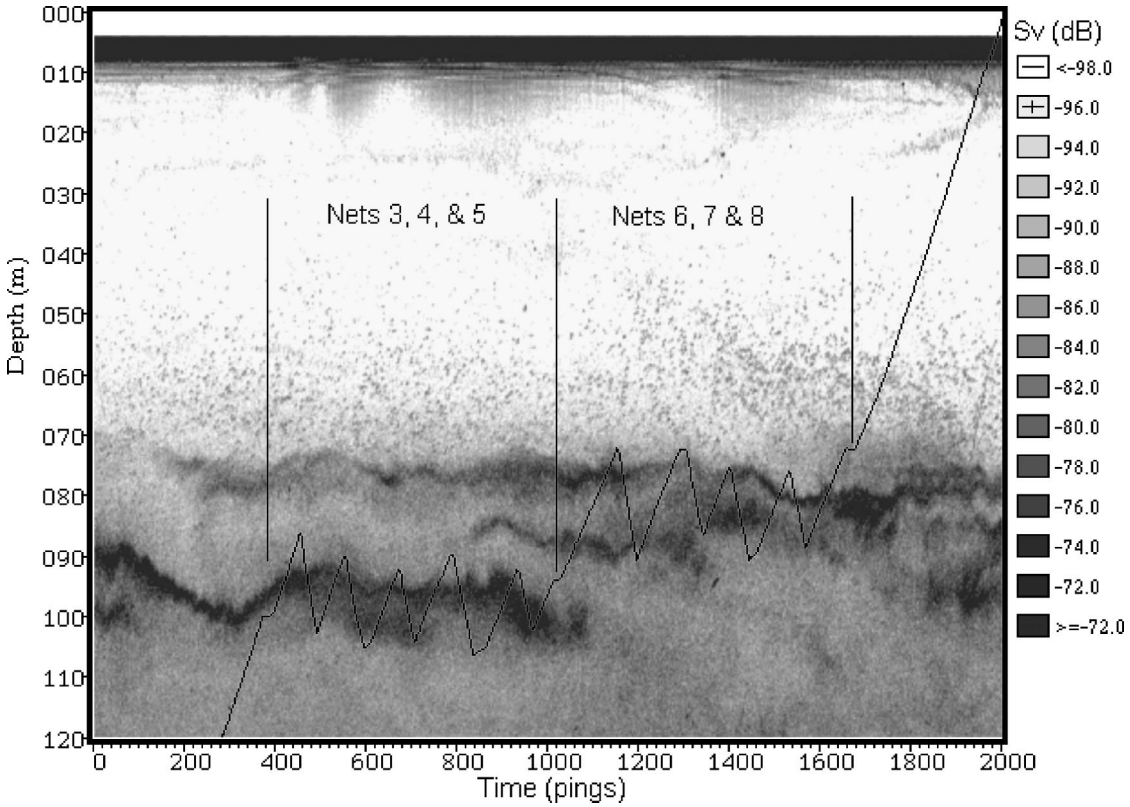

FIG. 2. Volumetric scatter strength vs depth and time at 120 kHz for 33.3 min starting 0833h, 23 Nov. 2002 near Shewell Island in Knight Inlet. Black line shows the trajectory of the BIONESS multinet sampler, with labels indicating zones of net opening.

IV. MULTIFREQUENCY ACOUSTIC RESULTS AND COMPARISONS WITH *IN SITU* DATA

For the purpose of examining the validity of the combined echo-sounder and *in situ* sampling approach, in essence verifying the use of the acoustic scattering models described above, six specific examples from the November 2002 surveys will be examined in detail. These examples are chosen for both the coincidence of good quality acoustic and BIONESS or ZOOVIS data, and the dominance of a particular zooplankton type or species.

A. Euphausiid aggregations in the lower inlet

Scattering layers dominated by euphausiids were commonly observed in the lower inlet and near the sill at Hoeya Head. A specific deep-water comparison between the echo-sounder and BIONESS results taken at 0830h 23 Nov. 2002 near Shewell Island will be examined here in detail. This example was chosen because it was located well away from the complicated, turbulent flows in the sill region, and because the net trawls indicated a moderate euphausiid abundance with only minor amounts of other species. ZOOVIS was not deployed at this site because earlier experiences had found very few euphausiids were imaged in these relatively low abundance layers.

Figure 2 presents a volumetric backscatter strength vs depth and time echogram, overlain with the trajectory of the BIONESS sampler (appropriately time shifted to compensate for the cable lay-back). The echogram shows the typical daytime scattering layer below roughly 70-m depth. The BIONESS acquired three nets in the lower sublayer at 85–105-m depth and three more nets within the upper sublayer at 72–90 m. Each net sampled between 50 and 80 m^3 within the zooplankton layer. Individual net results within each sublayer exhibited only minor differences, so euphausiid abundances vs size (1-mm size classes) were averaged over each set of three, with result presented in Fig. 3. The measured size distributions are clearly in agreement with the Gaussian-distributed assumption required for the averaged fluid cylinder scattering model described above. For modeling purposes a mean length of 15.9 mm and 1.4-mm standard deviation will be used. Also produced from BIONESS were

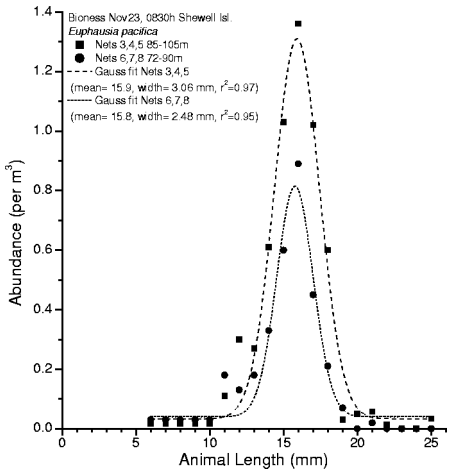

FIG. 3. Size-abundance distribution of *Euphausia pacifica* from BIONESS trawl at 0830h 23 Nov. 2002 near Shewell Island. Best-fit Gaussian distributions plotted as dashed and dotted lines for the two sublayers.

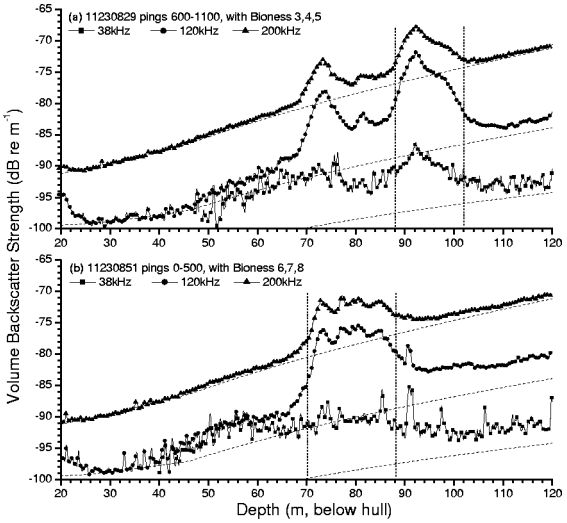

FIG. 4. S_v vs depth profiles at 38, 120, and 200 kHz, averaged over 500 pings (8.3 min) starting at (a) 0839h and (b) 0851h on 23 Nov. 2002 near Shewell Island. Depth-varying dashed lines are corresponding systemic noise levels for the three channels (S_v data are not corrected for noise). Vertical dashed lines show depth intervals of the corresponding BIONESS net trawls, found to be dominated by *E. pacifica* (as shown in Fig. 3).

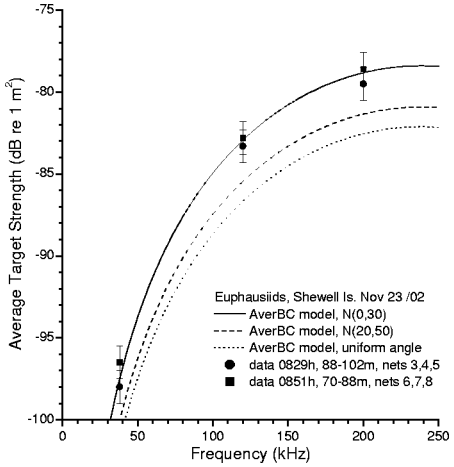

FIG. 5. Comparison between measured and predicted averaged target strength vs frequency for *E. pacifica* near Shewell Island, 0830h 23 Nov. 2002. Experimental TS derived from averaged S_v at 88–104 m and 72–90 m-depth divided by the mean abundance estimated from the BIONESS trawls. Error bars on TS are ± 0.8 dB. Predicted TS calculated from population- and orientation-averaged model using euphausiid length and standard deviation of 15.9 and 1.4 mm, respectively, with three different orientation angle distributions.

averaged total abundances of 5.6 and 3.2 euphausiids per m^3 for the lower and upper sublayers, respectively. This averaged abundance is considered low, as abundances in excess of 500 per m^3 were observed in other parts of the inlet. Finally, an examination of euphausiids captured at several sites in the lower inlet determined that the mean aspect ratio (length to width) was 7.6 ± 0.7. This implies a length to radius ratio of 15.2, similar to that reported for Antarctic krill (*E. superba*) by Foote *et al.*(1990) and Chu *et al.* (1993).

Averaged profiles of volume backscatter strength at the three frequencies for the two zooplankton sublayers are presented in Fig. 4. These volumetric backscatter cross-section profiles were ping averaged over the same interval as the BIONESS net samples shown in Fig. 2, and are uncorrected for systemic noise. These profiles exhibit the distinctive increasing scattering strength with frequency signature of euphausiid scattering layers. Specifically, the ratio between the scattering strength at 120 kHz to that at 38 kHz was approximately 14 dB, and between 200 and 120 kHz the ratio was roughly 4 dB. Within the euphausiid scattering layers the signal-to-noise ratios were generally good (>6 to 10 dB); however, the 200-kHz channel was increasingly noise dominated near the upper and lower boundaries of the euphausiid layers. In general, the 200-kHz channel was not useful for zooplankton sampling at depths >100 m. Note in Fig. 4(b) that the 38-kHz profile does not exhibit the same characteristic increase in scattering strength above the background as observed in the 120- and 200-kHz profiles. This is partly due to the inclusion in the averaged scattering level of echoes from a few larger, isolated targets in combination with low euphausiid signal level. The use of an upper threshold in the depth- and ping-averaging process removes much of this contamination. Quantitatively, within the lower sublayer [88–102 m in Fig. 4(a)], the noise-corrected depth-averaged volume scattering strengths were -90.5, -75.8, and -72.0 dB (*re*: 1 m^{-1}) at 38, 120, and 200 kHz, respectively. Similarly, in the upper sublayer [70–88 m in Fig. 4(b)] the noise-corrected depth-averaged S_v were -91.4, -77.7, and -73.5 dB.

By dividing the averaged volumetric scattering cross section by the measured abundance estimates from the BIONESS within each sublayer, estimates of the averaged target strength (TS, in dB *re*: 1 m^2) per animal at each frequency can be made (Fig. 5). Overall, there is good agreement in the TS estimates between the two sublayers at all three frequencies. Furthermore, there is excellent agreement between the TS estimates and the averaged bent fluid cylinder model prediction using a N(0°,30°) orientation distribution, and there is little overlap with either the N(20°,50°) or the uniform angular distribution predictions. These TS and orientation results are similar to those found for other naturally occurring euphausiid swarms, bearing in mind that most other studies were focused on larger euphausiids. For example, Wiebe *et al.* (1990) reported an average TS of -77.5 dB at 420 kHz for live, tethered, 20-mm-long *E. pacifica*. Foote *et al.* (1990) reported average TS for 34-mm-length *E. superba* near Antarctica in the range -89 to -85 dB at 38 kHz and -79 to -76 dB at 120 kHz. Foote's estimates are 8–12 dB larger at 38 kHz and 4–7 dB larger at 120 kHz for a mean animal size about twice these Knight Inlet euphausiids, entirely consistent with the present fluid-cylinder model using the larger animal size.

In terms of euphausiid orientation, these results are consistent with some previous studies. Based on *in situ* photographs of euphausiids in Norway, Kristensen and Dahlen (1986) reported a mean angle between $\pm 10°$ (dependent on vertical migration state) with standard deviation between 25° and 45°. They concluded that a $N(0°,30°)$ orientation distribution was appropriate for modeling purposes. However, in an examination of Antarctic krill data, Chu *et al.* (1993) extracted swimming angles with mean near 20° (head up) and standard deviation near 30°. Earlier photographic work

by Kils (1981) with Antarctic krill showed a mean orientation of 45° (head up) with a standard deviation of 30°. In tank experiments with similar-sized *E. pacifica*, Miyashita *et al.* (1996) reported typical swimming angle distributions with mean of 30° (head up) and standard deviation of 20°.

The BIONESS trawl data can also be used to assess the error due to scattering contributions from other species. Aside from euphausiids, the next most abundant zooplankton class was amphipods, with measured length distribution of 6.3 ± 2.4 mm and averaged abundance of 6.6 m^3 in both the lower and upper sublayers. Using a similar size and orientation-averaged scattering model (amphipod parameters are described in the next subsection), the predicted layer-averaged S_v values for amphipods are -100.5, -88.3, and -83.5 dB (*re*: 1 m^{-1}) at 38, 120, and 200 kHz, respectively. These are all more than 10 dB lower than the observed S_v attributed to euphausiids, and thus amphipod scattering can be guardedly ignored.

B. Amphipods in the western inlet

A combined acoustic and BIONESS survey at 1125h on Nov. 19, 2002 near Lady Island, in the western part of the lower inlet, found a situation dominated by amphipod scattering with almost negligible presence (abundance <0.1 per m^3) of euphausiids. During the BIONESS trawl, four individual nets were deployed within main scattering layer at 60–80-m depth, with an averaged abundance of 22.9 per m^3. Each net sampled between 80 and 100 m^3, so this abundance estimate is an average over roughly 330 m^3 of the scattering layer. There were two dominant species of amphipods, namely a hyperiid *Themisto pacifica* and a gammarid *Cyphocaris challengeri*. The combined size distribution of the hyperiid and gammarid amphipods was found to be Gaussian distributed with mean of 6.3 mm and standard deviation of 2.4 mm. The mean aspect (length-to-width) ratio measured from a number of amphipod samples was 5.2. ZOOVIS was not deployed at this site.

Ping-averaged volume backscatter strength profiles through this amphipod layer are presented in Fig. 6. Similar to euphausiid layers discusssed earlier, the three frequencies all exhibited a strong S_v signal within the 58–76-m amphipod layer and an increasing S_v with frequency. The noise-corrected depth- and ping-averaged S_v were -93.7, -83.2, and -79.0 dB (*re*: 1 m^{-1}) at 38, 120, and 200 kHz, respectively. As in the euphausiid case (Fig. 4), the 200-kHz profile had reasonable signal-to-noise properties within the amphipod scattering layers, but was clearly noise limited outside of the layer. Also, the ping-averaged 38-kHz S_v profile exhibited a different scattering texture, with rapid fluctuations in depth, both within and outside of the amphipod layer. This is in contrast to the more continuous, smooth scattering profiles of the 120- and 200-kHz channels. This contamination is due to the inclusion of echoes from a few isolated targets (identity unknown) in the averaged profile, made apparent by the small 38-kHz signature from amphipods. Again, the use of an upper threshold in the depth- and ping-averaging process removes much of this contamination.

Estimates of the averaged TS for these amphipods can be made by dividing the time- and depth-averaged volumetric backscatter cross section at each frequency by the measured abundance estimate from the BIONESS. Figure 7 compares the measured and modeled TS for this amphipod layer. In this case there is agreement with the model using a N(0°,60°) distribution, although the uniformly distributed case cannot be rejected. The 38-kHz estimate appears too high by roughly 2 dB, presumably due to residual contamination from these isolated scatterers mentioned above. Finally, we can use the upper bound on euphausiid abundance (0.1 per m^3) taken from the BIONESS trawl data to assess the potential interference with these amphipod S_v measurements. The fluid-cylinder model for euphausiids (discussed

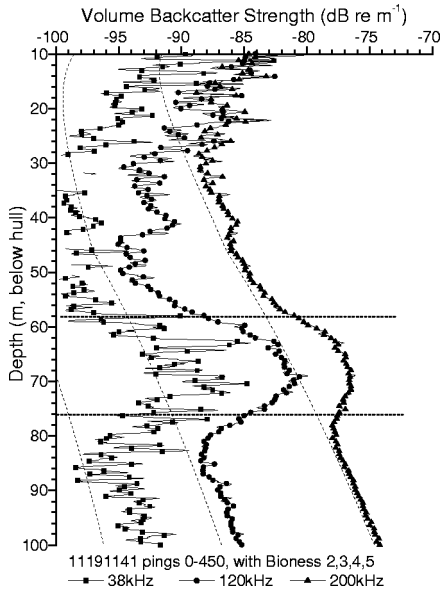

FIG. 6. S_v vs depth profiles at 38, 120, and 200 kHz, averaged over 450 pings (7.5 min) starting 1141h, 19 Nov. 2002 near Lady Island in Knight Inlet. Depth-varying dashed lines are corresponding systemic noise levels for the three channels (S_v data are not corrected for noise). Horizontal dashed lines show depth interval of the corresponding BIONESS net trawls, found to be dominated by hyperiid and gammarid amphipods.

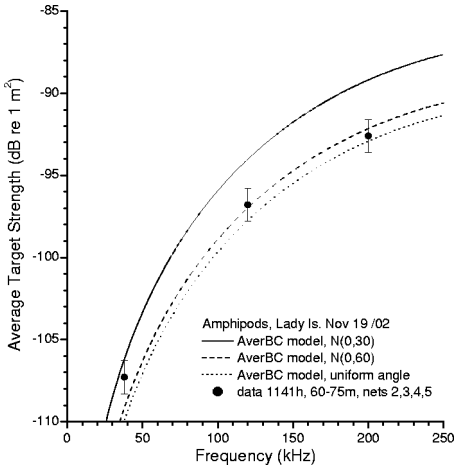

FIG. 7. Comparison between measured and predicted averaged target strength vs frequency for amphipods near Lady Island, 1141h 19 Nov. 2002. Experimental TS derived from averaged S_v at 60–78-m depth divided by the mean abundance estimated from the BIONESS trawl. Error bars on TS are ± 0.8 dB. Predicted TS calculated from population- and orientation-averaged model using amphipod length and standard deviation of 6.3 and 2.4 mm, respectively, with three different orientation angle distributions.

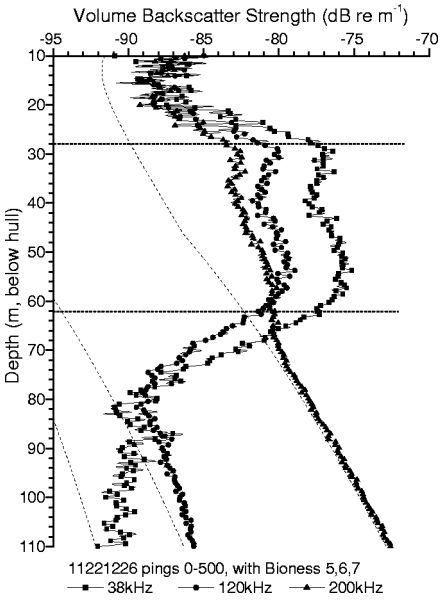

FIG. 8. S_v vs depth profiles at 38, 120, and 200 kHz, averaged over 500 pings (8.3 min) starting 1226h, 22 Nov. 2002 in Glacier Bay, Knight Inlet. Depth-varying dashed lines are corresponding systemic noise levels for the three channels (S_v data are not corrected for noise). Horizontal dashed lines show depth interval of the corresponding BIONESS net trawls, which showed presence of siphonophores and lack of euphausiids or amphipods.

above) predicts averaged S_v in this layer of -107.8, -93.1, and -88.9 dB (*re*: 1 m^{-1}) at 38, 120, and 200 kHz, respectively. These are all more than 11 dB below the observed S_v data for the amphipod scattering layer.

C. Siphonophores in Glacier Bay

Acoustic scattering signatures in the upper inlet were found to be drastically different from those found in the lower inlet. In this case the scattering strength vs frequency trend was reversed, with the 38 kHz being the strongest and the 200 kHz the weakest, as demonstrated in Fig. 8 with an example from midday on 22 Nov. 2002. Clearly, all three echo-sounders were able to resolve the scattering layer with moderate to good signal-to-noise ratios. Focusing on a region near the upper boundary of this layer (28–32 m), the noise-corrected depth- and ping-averaged S_v were -77.1, -80.5, and -83.8 dB (*re*: 1 m^{-1}) at 38, 120, and 200 kHz, respectively. A simultaneous BIONESS trawl from 30–65-m depth detected the presence of siphonophore (identified as *Nanomia bijuga*) nectophores, pneumatophores, and siphonulae. Specifically, within this 30–65-m layer the averaged abundances of nectophores and pneumatophores from BIONESS were 1.29 and 0.13 per m^3, respectively. Since it is reasonable to expect roughly 10 nectophores per *Nanomia* colony but only one pneumatophore, these two estimates are consistent. The trawls also found a distinct absence of euphausiids and amphipods in this layer (averaged euphausiid and amphipod abundances were <0.15 and 0.4 per m^3, respectively). Using the euphausiid and amphipod TS outlined in previous sections, these measured abundances predict scattering strengths that are much smaller than observed, particularly for the 38-kHz channel. ZOOVIS was deployed at this site prior to the BIONESS cast, but did not return any siphonophore images due to the low abundances.

Because of the relative fragility of the siphonophore colonies and their relatively low abundance, standard net trawls (such as BIONESS) are considered somewhat unreliable for measuring siphonophore abundance. Fortunately, an alternate estimate of the average target strength can be derived from an examination of the scattering layer statistics, using a technique outlined in Stanton (1985) and used by Trevorrow and Tanaka (1997) to estimate *in situ* amphipod TS. The basis of this technique, dubbed *critical density analysis*, is that probability density functions of scattering amplitude show different shapes between the two extremes of overlapping and nonoverlapping scatterer echoes. The transition between these two extremes, which is generally rather sharply defined in depth and easy to identify from PDF shape, corresponds to a depth where *on average* there is one scatterer per insonified volume (i.e., a *critical* density). With knowledge of the averaged S_v at this depth of critical density, the average backscatter cross section (i.e., TS) can be extracted.

In the specific example examined here, critical density points for the 38- and 120-kHz channels were found at 29.4-m depth. The corresponding critical densities were 0.162 m^{-3} for both channels, with noise-corrected, ping-averaged S_v of -76.2 and -80.3 dB (*re*: 1 m^{-1}), at 38 and 120 kHz, respectively. Combining the critical density and average scattering strength produced averaged TS estimates of -68.3 and -72.4 dB (*re*: 1 m^2) at 38 and 120 kHz, respectively. A TS estimate at 200 kHz of -75.1 dB was generated using the ratio between layer-averaged S_v at 38 and 200 kHz (-6.8 dB). A similar critical density point was found in the 38-kHz channel at the bottom of the layer (75-m depth), yielding at 38 kHz TS of -68.4 dB (*re*: 1 m^2). Using ratios between averaged S_v at the three frequencies near 75-m depth, the estimated TS at 120 and 200 kHz at this depth was -72.3 and -75.1 dB (*re*: 1 m^2), respectively. A similar critical density analysis performed on a separate data set taken earlier (1020h) on the same day in a nearby location produced similar results (e.g., averaged TS$=-69.1$, -73.1, and -75.5 dB at 38, 120, and 200 kHz at 30-m depth).

Using these TS values, the average siphonophore abundance was near 0.14 per m^3, very close to the abundance estimated from the nectophores and pneumatophores captured in the BIONESS trawl. Similar abundances (mean of 0.05 per m^3, maximum up to 1 per m^3) of *Nanomia bijuga* in Monterey Bay were reported by Robison *et al.* (1998) from ROV-based video observations. However, these present estimates are considerably lower than 1–10 siphonophores per m^3 estimated acoustically for *N. cara* in the Gulf of Maine reported by Warren *et al.* (2001), Benfield *et al.* (2003b), and earlier submersible observations in the same Gulf of Maine region by Rogers *et al.* (1978).

A comparison between these TS estimates and siphonophore scattering models is presented in Fig. 9. Because the scattering model for a bubble (our model for a pneumatophore) is depth dependent, the figure presents comparisons at 30 and 60-m depth, near the upper and lower boundaries of

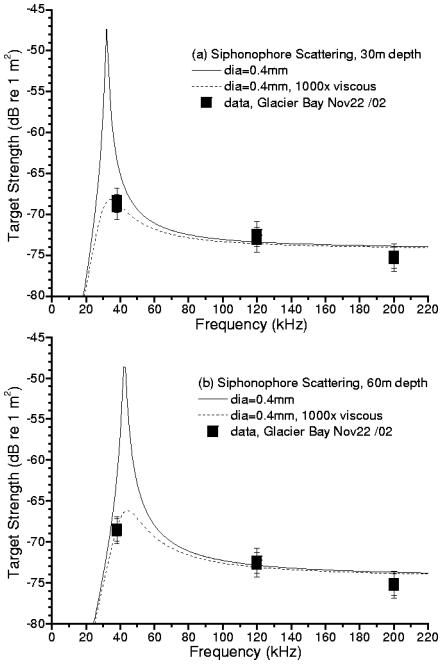

FIG. 9. Comparison between measured and predicted averaged target strength vs frequency for siphonophores in Glacier Bay, Knight Inlet. Experimental TS derived from critical density analysis (as described in the text) from data at 1017h and 1226h, 22 Nov. 2002. Error bars on TS are ± 1.5 dB.

the siphonophore layer. The bubble model clearly exhibits a resonant peak near 40 kHz, and that this resonant frequency increases with depth. The best overall fit at frequencies above the resonance (i.e., 120 and 200 kHz) comes for a 0.4-mm bubble diameter. However, for this size the unmodified bubble model overpredicts the measured TS at 38 kHz at both 30 and 60 m. A better fit to the 38-kHz TS at both depths can be found by arbitrarily increasing the viscous damping component by a factor of 1000. Furthermore, note that at 30-m depth the resonant peak is below the 38-kHz echo-sounder frequency, while at 60-m depth the resonance is above 38 kHz. Assuming the pneumatophore size to be roughly uniform throughout this layer, the unmodified bubble model predicts that a strong resonant scattering region, roughly 20 dB higher, should occur in the 38-kHz channel at some intermediate depth. From Eq. (4), a 0.4-mm-diameter bubble has a predicted 38-kHz resonance at a depth of 45 m. Examination of Fig. 8 indicates that the ratio of S_v between 38 and 120 kHz is approximately constant from 30- to 60-m depth, with no suggestion of a resonant peak near 45 m. These facts lend support to the earlier hypothesis that the membrane surrounding the gas bubble in the pneumatophore adds damping. However, the exact damping contributions are difficult to assess except under carefully controlled laboratory conditions. This 0.4-mm pneumatophore diameter lies in between adult pneumatophore sizes of 0.7–1.0 mm examined in Warren *et al.* (2001), and siphonulae pneumatophore diameters of 0.1-0.4 mm found by Benfield *et al.* (2003). Furthermore, these present measurements are consistent with previous siphonophore TS measurements. For example, Warren *et al.* reported average TS measurements of -62.5 dB at 24 kHz, while Benfield *et al.* predicted average TS of -72 dB at 120 kHz and -77 dB at 200 kHz. Independently, Greene *et al.* (1998) reported a siphonophore TS of -75 dB at 420 kHz based on direct acoustic vs net trawl comparisons in the Gulf of Maine.

D. Echo-sounder vs ZOOVIS comparisons

The occurrence of dense euphausiid scattering layers in the lower inlet also allowed closely coupled comparisons between the echo-sounders and ZOOVIS. For these comparisons, 120-kHz volume scatter strength can be converted to euphausiid abundances using results from Sec. IV A, specifically using a mean TS of -83.1 dB (*re*: 1 m^2). The 120-kHz channel is used as it provided the best overall signal-to-noise performance for the euphausiid layers. However, in contrast to the BIONESS comparisons where time- and depth averages were appropriate, comparisons to the small sample volume of ZOOVIS (of order 1 liter) requires high-resolution acoustic data. For this analysis the echo-sounder data were averaged over two successive pings (2 s) and into 24-cm-depth bins. Figure 10 presents a detailed ZOOVIS vs acoustic comparison for a shoaling near-surface euphausiid layer near Lady Island. Typical acoustically derived abundances in this example are 100 to 200 per m^3, with isolated patches exceeding 500 per m^3. The maximum acoustically predicted abundance is 775 per m^3. Note that the insonified volume of the 120-kHz echo-sounder increases with depth from 0.6–4.3 m^3 within this 8–22-m deep layer, approximately 10^3 to 10^4 times larger than the sample volume of ZOOVIS (0.36 liter in this deployment). The ZOOVIS-derived abundances are based simply on counting the number of recognizable euphausiid targets per image, then dividing by the sample volume. Note that the minimum quantity of 1 euphausiid per image corresponds to an abundance of 2.8 per liter (2800 per m^3), much larger than any observed with the echo-sounder. In this example no more than 1 euphausiid per image was observed, and the majority of images was empty. The overall average ZOOVIS abundance from this deployment was 0.427 per liter. Generally, there is reasonable agreement in the sense that high ZOOVIS abundances correspond to locations where the instrument profiled through denser acoustic regions, and empty ZOOVIS images come from zones with low acoustic abundance.

Overall the ZOOVIS abundances presented in Fig. 10 appear to be about 2 to 4 times higher than the acoustic estimates. There are a number of possible contributing factors to this discrepancy. First, the huge difference in sampling volumes implies different sampling statistics for the two measurements, one being an average over many targets per insonified volume and other having only isolated hits. However, the average ZOOVIS abundance (including zero estimates) is still about a factor of 2 larger than the typical acoustic abundances. Another complication is that of animal swimming-angle orientation. If the euphausiids had a different orientation distribution, say closer to uniformly distributed, then their average TS could be plausibly lower by as much as 3 dB (see Fig. 5). Some evidence for this can be seen from an oblique bongo net trawl over the upper 30 m taken roughly 1 h later at this same Lady Island site. The

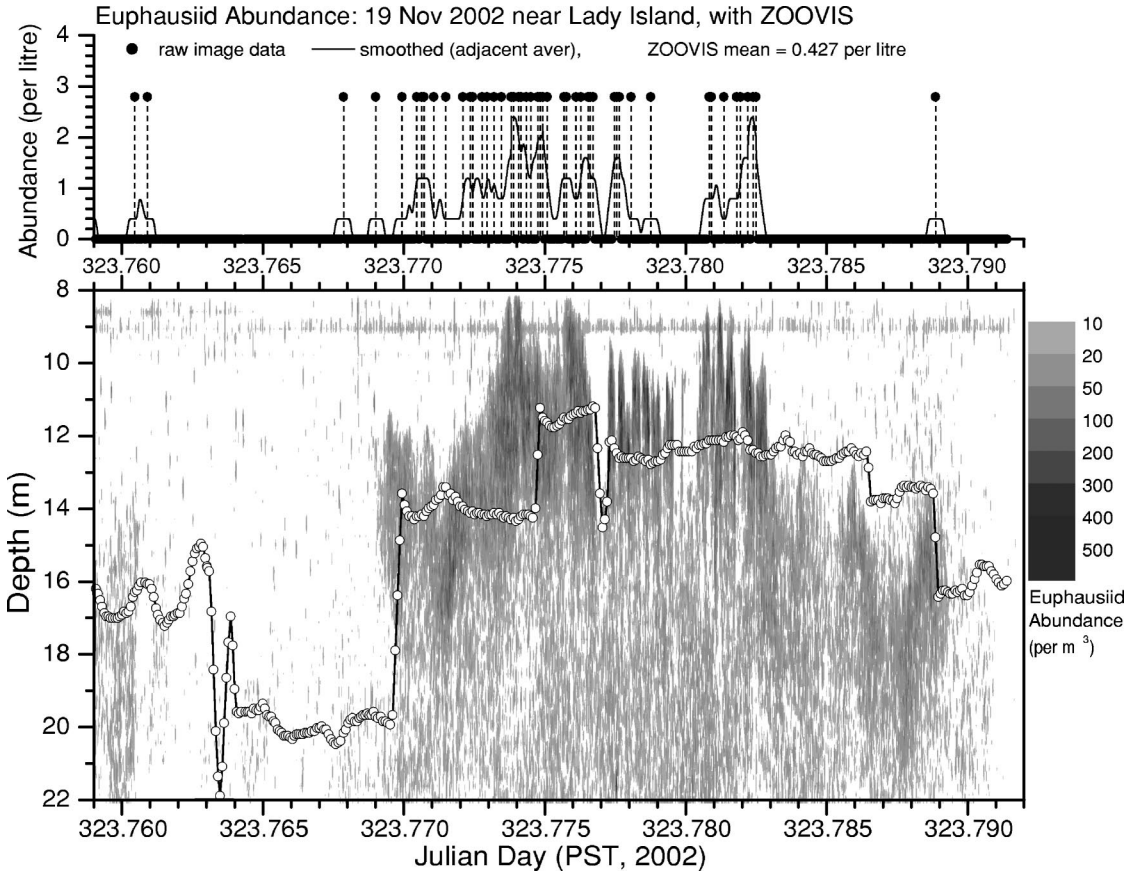

FIG. 10. Comparison of echo-sounder and ZOOVIS abundance time-series, 1812h to 1900h 19 Nov. 2002 near Lady Island. Upper panel shows ZOOVIS abundances (per liter) based on a 0.36-liter sampling volume. Smoothed curve is a 7-point adjacent average. Lower panel shows echo-sounder abundance (per m^3) vs depth and time calculated from 120-kHz echo-sounder assuming 15.9-mm-length euphausiids as described in Sec. IV A. Echo-sounder data has 2-s time and 24-cm depth resolution. ZOOVIS trajectory overlain on echo-sounder contour plot, with circles indicating individual images.

bongo picked up the usual 15.9-mm length euphausiids, with a layer-averaged abundance of 23.5 per m^3. Averaged over the same depth and time interval as the bongo trawl, the acoustically derived abundance estimate (based on the same methods as for the ZOOVIS comparisons) was 16.5 per m^3. This suggests that the average euphausiid TS could be smaller by 1.5 dB, potentially pushing the acoustically derived abundances in Fig. 10 upwards by roughly 50%. A final complication is that this region clearly exhibited high spatial heterogeneity, and it is possible that ZOOVIS was towed through slightly different euphausiid swarms than sampled by the echo-sounder. The difference between the two sampling points was roughly 30-m distance and 20 s in time.

Figure 11 presents another, deeper acoustic vs ZOOVIS comparison near the Hoeya Head sill. This example contains some of the highest euphausiid densities observed during the Nov. 2002 field trail. Acoustically, the typical peak abundance was 200 to 400 per m^3 with several patches in excess of 1000 per m^3. The maximum acoustically derived abundance was 1610 per m^3 for the patch at JD=327.659 and 77-m depth. At these greater depths the acoustically insonified volumes were 32–45 m^3, again roughly 10^4 times larger than the ZOOVIS sample volume (3.4 liters). In this deployment the minimum observable ZOOVIS abundance was 0.29 per liter, and there were several images with multiple euphausiids (up to 8 in one image). The overall average ZOOVIS abundance was 0.36 per liter, in rough agreement with the acoustic estimates, and there is reasonable correlation in the locations of abundance peaks. However, the peak ZOOVIS values (up to 3400 per m^3) were approximately a factor of 2 larger than the acoustics. Due to the increased flow-induced turbulence near the Hoeya Head sill, it is plausible that the euphausiids could have had a different swimming-angle distribution, likely closer to uniformly distributed. This effect could reduce the average TS by roughly 3 dB, effectively doubling the acoustically derived abundance. Additionally, there was a larger spatial separation of the acoustic and ZOOVIS samples created by the greater length of cable required to deploy ZOOVIS to this depth. The estimated separation was roughly 80-m distance and 52 s in time, increasing the potential sampling mismatch.

E. Effects of vessel lights on near-surface euphausiids at night

A dramatic example of euphausiid reaction to light was found during a nighttime survey near the Hoeya Head sill on 21 Nov. 2002. At this time the vessel was moving slowly during a deployment of ZOOVIS. When the aft-deck flood lights were turned on, the euphausiid scattering layer near 20-m depth suddenly dropped in intensity by roughly 10–15 dB, depending on frequency. This change in the scattering layer was found to be repeatable by alternating 2-min periods with the lights on and off. Figure 12 compares scattering

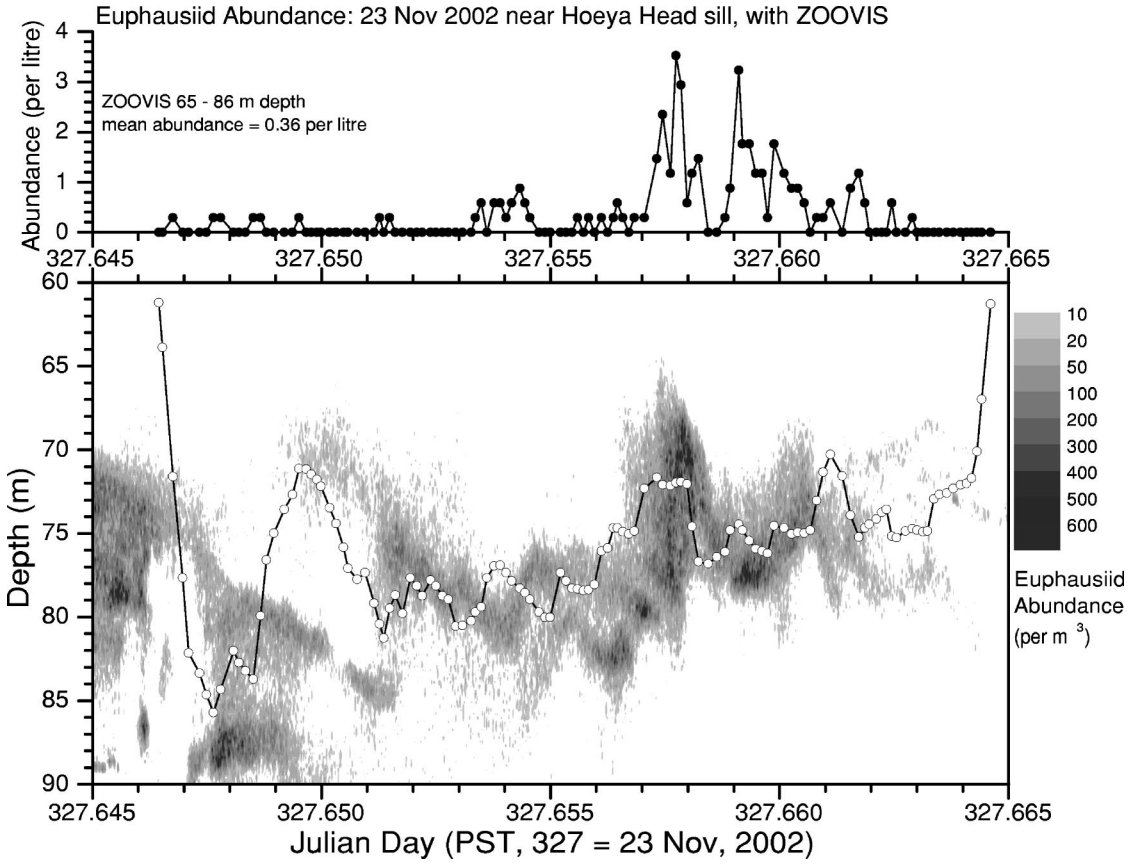

FIG. 11. Comparison of echo-sounder and ZOOVIS abundance time-series, 1528h to 1557h 23 Nov. 2002 near Hoeya Head sill. Upper panel shows ZOOVIS abundances (per liter) based on a 3.41-liter sampling volume. Lower panel shows echo-sounder abundance (per m^3) vs depth and time calculated from 120-kHz echo-sounder assuming 15.9-mm-length euphausiids as described in Sec. IV A. Echo-sounder data have 2-s time and 24-cm depth resolution. ZOOVIS trajectory overlain on echo-sounder contour plot, with circles indicating individual images.

strength profiles averaged over 1-min intervals immediately before and after the lights were turned on. In this example there were two scattering layers, one at 6–9 m and the other at 17–26-m depth. With the lights off, the averaged scattering strength within layer 2 is consistent with euphausiids (as described above) with average density of 6.6 per m^3. When the lights were turned on there was a clear decrease in S_v in layer 2. In the shallower portion of layer 2 (at 17–21-m depth) the depth- and ping-averaged scattering strength decreased by 9.8 and 10.8 dB at 120 and 200 kHz, respectively. Since this decrease was sudden (occurring within a few seconds), the euphausiids could not have had time to swim down, but rather must have simply changed their swimming-angle orientation. Since this magnitude is much larger than can be accounted for by going from a near-horizontal to a uniformly distributed swimming angle (which is about 5 dB; see Fig. 5), the most likely explanation is that the euphausiids have turned from near-dorsal to near-vertical incidence (either head or tail up). Since there is a suggestion in the *Lights On* profile that some part of scattering layer 2 has migrated downward to almost 35 m, a likely explanation is that these euphausiids have turned to swim downwards. Sameoto (1993) observed similar euphausiid photosensitivity to strobe lights mounted on a BIONESS. Interestingly, the zooplankton scattering strength in layer 1, much nearer the ship and the surface, actually increased by approximately 1.5 dB during the same period.

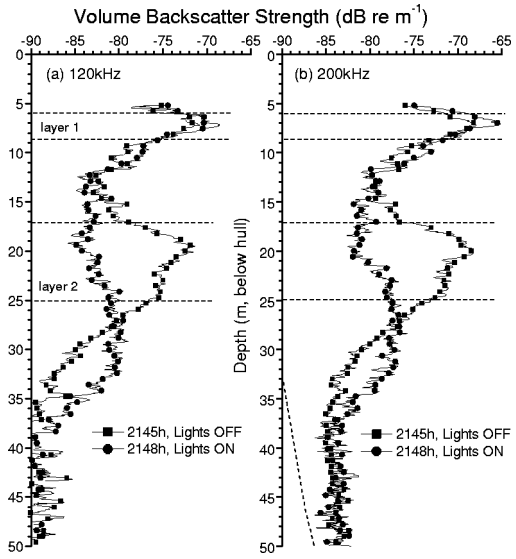

FIG. 12. Comparison of S_v vs depth profiles at (a) 120 and (b) 200 kHz, showing effects of light on euphausiids at night. Each profile averaged over 60 pings (1 min) starting at 2145h and 2148h on 21 Nov. 2002 near the sill at Hoeya Head. Depth-varying dashed line in (b) is the 200-kHz systemic noise level. Horizontal dashed lines identify two distinct scattering layers.

V. DISCUSSIONS AND CONCLUSIONS

Overall, this study showed the necessity of combining multifrequency acoustic backscatter with *in situ* net and op-

tical samples. The echo-sounders offered greater coverage rate and relatively high resolution, particularly in the fact that they sampled surface-to-seabed nearly instantaneously. The strength of the *in situ* samplers was clearly the ability to identify species and quantify size and average abundance. What emerged is an approach where the echo-sounders were employed as a spatial and temporal bridge between the isolated *in situ* samples. In these surveys the echo-sounder frequencies of 38, 120, and 200 kHz provided good coverage of the acoustically relevant portion of the zooplankton scattering spectrum, while at the same time providing reasonable sensitivity to depths of 100 to 200 m. A clear requirement for the echo-sounders was an acoustic calibration, specifically including on-axis sensitivity, beam pattern, time-varying gain curves, and instrumental noise limits.

By closely coupling the acoustic vs BIONESS comparisons through relatively homogeneous and mono-specific zooplankton scattering layers, acoustic scattering models for crustacean zooplankton and siphonophores could be validated. In particular, the echo-sounder observations of euphausiid and amphipod scattering layers satisfied a number of assumptions in the averaged fluid-cylinder model, namely the superposition of echoes from a large number of animals, a Gaussian-distributed size distribution (e.g., Fig. 3), and the dominance of a single scatterer type. The comparisons were aided by the fact that the BIONESS and acoustic sample volumes (roughly 50 to 100 m^3) were approximately matched. Furthermore, the ability to steer BIONESS to specific depths, allowing samples of particular scattering layers, greatly facilitated the comparisons. Overall, for crustacean scattering the agreement between observed and modeled TS at 120 and 200 kHz was excellent. Additionally, averaged TS and swimming orientation estimates were largely consistent with those previously reported in the literature. Unfortunately, in most situations encountered in this study the zooplankter abundances were too low to enable ZOOVIS to adequately sample the *in situ* orientation distributions. It was found that measurements at 38 kHz were occasionally contaminated by nonzooplankton echoes, particularly for cases of low euphausiid abundances and for the amphipod scattering. This contamination was readily identified in the S_v profiles as a spiky, irregular depth variation as opposed to the relatively smooth profiles exhibited by the 120- and 200-kHz channels (i.e., the echo-amplitude statistics would be different). This contamination appeared for regions with observed S_v less than roughly -90 dB (*re*: m^{-1}). The use of an upper threshold in echo-averaging largely removed this contamination.

The euphausiid and amphipod scattering examples were best modeled using a mean swimming angle of zero (horizontal), with a standard deviations of 30° and 60°, respectively. The euphausiid swimming-angle distribution was similar to some previously reported distributions for nonmigratory, *in situ* euphausiid swarms. Kristensen and Dahlen (1986) suggested that during vertical migrations the euphausiids varied their mean swimming angle by $\pm 10°$, but that a zero mean angle and 30° standard deviation was appropriate for modeling purposes. The *in situ* measurements on Antarctic krill reported by Kils (1981), which predicted a mean swimming angle of 45° (head up), and those of Chu *et al.* (1993), which predicted mean swimming angles near 20°, may not be applicable simply due to the different species and environment. In the example discussed in Sec. IV A, the euphausiids were clearly in a deep daytime, stationary layer. It is quite possible that they could have a different mean orientation during migration events or nocturnal foraging. Additionally, Chu *et al.* suggest that inversion of multifrequency data for the *in situ* swimming orientation might be possible. However, in most of the cases examined herein insufficient zooplankton samples were collected with ZOOVIS to establish reliable swimming orientation distributions.

Two examples were presented where the acoustic effects of zooplankter orientation were thought to be significant. In a nighttime near-surface survey the presence or absence of ship deck lights produced near-instantaneous changes in volume scatter strength by up to 15 dB. Since this change occurred within a few seconds, the euphausiids could not have had time to actively swim away, but rather must have simply changed their swimming-angle orientation. This change in volume scattering strength was significantly larger than predicted by a change of orientation from near-horizontal to uniformly distributed, and indicates a probable shift to near-tail incidence. This change was also larger than could be accounted for by the $\pm 10°$ variation in mean swimming angle suggested by Kristensen and Dahlen (1986). Unfortunately, the averaged fluid-cylinder model proposed by Stanton and Chu (2000) is only valid near lateral incidence. There is a clear need for these models to be extended for head or tail incidences. Another example showing the influence of zooplankter orientation comes from the acoustic vs ZOOVIS comparisons for the dense euphausiid layers near the turbulent flows at the Hoeya Head sill. The acoustically derived abundances were consistently about a factor of 2 lower than average abundances extracted from ZOOVIS. The can be at least partially explained by a change in swimming orientation distribution, from near-horizontal to more uniformly distributed. An investigation of euphausiid orientation distributions gleaned from ZOOVIS images in the higher-abundance regions is clearly called for.

The observations of siphonophore scattering in the upper inlet were unexpected. The siphonophore scattering signature exhibited a *reversed* scattering strength vs frequency, i.e., with the 38-kHz volume scattering the highest and 200 kHz the lowest. Because of the fragility of these gelatinous colonies, only isolated nectophores, pneumatophores, and siphonulae were recovered with BIONESS. An acoustic technique based on echo-amplitude statistics was used to extract siphonophore abundances and TS, producing reasonable estimates. The acoustically derived siphonophore abundance (near 0.15 per m^3) was consistent with the net samples. Similar to previous studies, the siphonophore scattering was found to be consistent with a damped bubble scattering model. The observed TS at 120 and 200 kHz was best fit by a 0.4-mm-diameter bubble size, similar to pneumatophore diameters reported by other investigators. However, at frequencies near 38 kHz the simple bubble model showed a strong resonance, generally overpredicting the observed TS by approximately 5 to 10 dB. Given the fact that the modeled

resonant peak exceeds the high-frequency TS by more than 30 dB, this discrepancy is not unreasonable. However, a suggestion for enhanced viscous damping by the pneumatophore membrane could be seen from two features in the 38-kHz scattering signature: (i) the apparent agreement at 38 kHz with a modified bubble model with 1000 times greater viscous damping, and (ii) the lack of a resonant peak in the 38-kHz S_v profile near 45 m depth. Clearly, this issue of pneumatophore damping would benefit from a careful laboratory investigation focused on the near-resonance region.

An interesting feature of echo-sounder vs ZOOVIS comparisons was the large difference in the sampling volumes of the two sensors (roughly a factor of 10^4). In its present configuration, the sampling rate and resolution of the camera were limited to 0.125–0.2 Hz and sampling volumes of 0.3 to 3.4 liters. In this work, ZOOVIS estimates of euphausiid abundances generally exceeded acoustically derived estimates by a factor of 2–4. In addition to issues surrounding zooplankter orientation discussed above, we believe that this mismatch in the sampling volumes potentially explains some of this difference. To test the effects of sample volume, a simple numerical model was created. In this model, a randomized distribution of a large number of particles (10^5) with known average density was generated. Then, a test sample volume was moved through this field of particles and the numerical density was calculated over a limited number of trials (500), simulating multiple echo-sounder pings or ZOOVIS images. The relevant parameter here is the size of the sample volume relative to the *critical volume*, defined as the reciprocal of the average particle density. For larger, supercritical sample volumes the distribution of estimated particle densities was narrowly distributed around the true average density, with the distributions increasingly narrow with larger sampling volumes. However, for very small sampling volumes ($<1\%$ of the critical volume), the distribution of estimated particle densities was bimodal, with a large number of zero estimates and a significant number of large overestimates. For a limited number of trials in the small sample volume case (i.e., modeling the ZOOVIS data collection), the overall mean density was found to be biased high by up to a factor of 3. This simple modeling suggests then that estimates of mean particle density will depend on the relative criticality of the sample volume and the number of samples. Additionally, natural zooplankton layers generally exhibit spatial *patchiness*, and thus some dependence on sampling volume size relative to patch size should be expected. Clearly, more work on the statistics of small volume samplers should be performed.

ACKNOWLEDGMENTS

This work was supported by grants from the US Office of Naval Research, Biological and Chemical Oceanography (Dr. Jim Eckman). BIONESS surveys and postanalyses were ably handled by Doug Yelland, Moira Galbraith, and Doug Moore, all of the Institute of Ocean Sciences. Finally, the authors are grateful for the skill and hard work from the officers and crew of the *CCGS* VECTOR during the two field trips in 2001 and 2002.

Benfield, M., Schwehm, C., Fredericks, R., Squyres, G., Keenan, S., and Trevorrow, M. (**2003a**). "ZOOVIS: A high-resolution digital still camera system for measurement of fine-scale zooplankton distributions," in *Scales in Aquatic Ecology: Measurement, Analysis and Simulation*, edited by P. Strutton and L. Seuront (CRC Press, Boca Raton, FL).

Benfield, M., Lavery, A., Wiebe, P., Greene, C., Stanton, T., and Copley, N. (**2003b**). "Distributions of physonect siphonulae in the Gulf of Maine and their potential as important sources of acoustic scattering," Can. J. Fish. Aquat. Sci. **60**, 0759–772.

Chu, D., Foote, K., and Stanton, T. (**1993**). "Further analysis of target strength measurements of Antarctic krill at 38 and 120 kHz: Comparison with deformed cylinder model and inference of orientation distribution," J. Acoust. Soc. Am. **93(5)**, 2985–2988.

Farmer, D., and Armi, L. (**1999a**). "The generation and trapping of solitary waves over topography," Science **283**, 188–190.

Farmer, D., and Armi, L. (**1999b**). "Stratified flow over topography: The role of small-scale entrainment and mixing in flow establishment," Proc. R. Soc. London, Ser. A **455**, 3221–3258.

Foote, K., Everson, I., Watkins, J., and Bone, D. (**1990**). "Target strengths of Antarctic krill (*Euphausia superba*) at 38 and 120 kHz," J. Acoust. Soc. Am. **87(1)**, 16–24.

Francois, R., and Garrison, G. (**1982**). "Sound absorption based on ocean measurements II. Boric acid contribution and equation for total absorption," J. Acoust. Soc. Am. **72**, 1879–1890.

Greene, C., Wiebe, P., and Burczynski, J. (**1989**). "Analyzing zooplankton size distributions using high-frequency sound," Limnol. Oceanogr. **34(1)**, 129–139.

Greene, C., Wiebe, P., Pershing, A., Gal, G., Popp, J., Copley, N., Austin, T., Bradley, A., Goldborough, R., Dawson, J., Hendershott, R., and Kaartvedt, S. (**1998**). "Assessing the distribution and abundance of zooplankton: A comparison of acoustic and net-sampling methods with D-BAD MOCNESS," Deep-Sea Res., Part II **45**, 1219–1237.

Greenlaw, C. (**1979**). "Acoustical estimation of zooplankton populations," Limnol. Oceanogr. **24(2)**, 226–242.

Harrison, P., Fulton, J., Taylor, F., and Parsons, T. (**1983**). "Review of the biological oceanography of the Strait of Georgia: Pelagic environment," Can. J. Fish. Aquat. Sci. **40**, 1064–1094.

Holliday, D. V., and Pieper, R. (**1980**). "Volume scattering strengths and zooplankton distributions at acoustic frequencies between 0.5 and 3 MHz," J. Acoust. Soc. Am. **67(1)**, 135–146.

Holliday, D. V., and Pieper, R. (**1993**). "Bioacoustical oceanography at high frequencies," ICES J. Mar. Sci. **52**, 279–296.

Johnson, R. (**1977**). "Sound scattering from a fluid sphere revisited," J. Acoust. Soc. Am. **61**, 375–377.

Kils, U. (**1981**). "The swimming behavior, swimming performance, and energy balance of Antarctic krill, *Euphausia superba*," BIOMASS Sci. Ser. **3**, 122 pp.

Klymak, J., and Gregg, M. (**2001**). "Three-dimensional nature of flow near a sill," J. Geophys. Res. **106(C10)**, 22295–22311.

Klymak, J., and Gregg, M. (**2003**). "The role of upstream waves and downstream density pool in the growth of lee waves: Stratified flow over the Knight Inlet sill," J. Phys. Oceanogr. **33**, 1446–1461.

Klymak, J., and Gregg, M. (**2004**). "Tidally generated turbulence over the Knight Inlet sill," J. Phys. Oceanogr. **34(5)**, 1135–1151.

Kristensen, A., and Dahlen, J. (**1986**). "Acoustic estimation of size distributions and abundance of zooplankton," J. Acoust. Soc. Am. **80(2)**, 601–611.

Korneliussen, R. (**2000**). "Measurement and removal of echo integration noise," ICES J. Mar. Sci. **57(4)**, 1204–1217.

Mackie, G., and Mills, C. (**1983**). "Use of the Pisces IV submersible for zooplankton studies in coastal waters of British Columbia," Can. J. Fish. Aquat. Sci. **40**, 763–776.

Mackie, G. (**1985**). "Midwater macroplankton of British Columbia studies by submersible PISCES IV," J. Plankton Res. **7(6)**, 753–777.

Medwin, H., and Clay, C. (**1998**). *Fundamentals of Acoustical Oceanography* (Academic, San Diego).

Miyashita, K., Aoki, I., and Inagaki, T. (**1996**). "Swimming behavior and target strength of Isada krill (*Euphausia pacifica*)," ICES J. Mar. Sci. **53**, 303–308.

Robison, B., Reisenbichler, K., Sherlock, R., Silguero, J., and Chavez, F. (**1998**). "Seasonal abundance of the siphonophore *Nanomia bijuga* in Monterey Bay," Deep-Sea Res., Part II **45**, 1741–1751.

Rogers, C. (**1978**). "Aggregation of the siphonophore *Nanomia cara* in the

Gulf of Maine: Observations from a submersible,'' Fish. Bull. **76**, 281–284.
Ross, T., and Lueck, R. (**2003**). ''Sound scattering from oceanic turbulence,'' Geophys. Res. Lett. **30**, 1344–1347.
Sameoto, D., Jarozynski, L., and Fraser, W. (**1980**). ''BIONESS: A new design in multiple net zooplankton samplers,'' Can. J. Fish. Aquat. Sci. **37**, 722–724.
Sameoto, D., Cochrane, N., and Herman, A. (**1993**). ''Convergence of acoustic, optical, and net-catch estimates of euphausiid abundance: use of artificial light to reduce net avoidance,'' Can. J. Fish. Aquat. Sci. **50(2)**, 334–346.
Stanton, T. (**1985**). ''Density estimates of biological sound scatterers using sonar echo peak PDFs,'' J. Acoust. Soc. Am. **78(5)**, 1868–1873.
Stanton, T. (**1989**). ''Simple approximate formulas for backscattering of sound by spherical and elongated objects,'' J. Acoust. Soc. Am. **86(4)**, 1499–1510.
Stanton, T., Chu, D., Wiebe, P., and Clay, C. (**1993**). ''Average echoes from randomly oriented random-length finite cylinders: Zooplankton models,'' J. Acoust. Soc. Am. **94(6)**, 3463–3472.
Stanton, T., Wiebe, P., Chu, D., and Goodman, L. (**1994**). ''Acoustic characterization and discrimination of marine zooplankton and turbulence,'' ICES J. Mar. Sci. **51**, 469–479.
Stanton, T., Chu, D., Wiebe, P., Martin, L., and Eastwood, R. (**1998**). ''Sound scattering by several zooplankton groups. I. Experimental determination of dominant scattering mechanisms,'' J. Acoust. Soc. Am. **103(1)**, 225–235.
Stanton, T., and Chu, D. (**2000**). ''Review and recommendations for the modeling of acoustic scattering by fluid-like elongated zooplankton: Euphausiids and copepods,'' ICES J. Mar. Sci. **57**, 793–807.
Trevorrow, M., and Tanaka, Y. (**1997**). ''Acoustic and *in situ* measurements of freshwater amphipods (*Jesogammarus annandalei*) in Lake Biwa, Japan,'' Limnol. Oceanogr. **42(1)**, 121–132.
Trevorrow, M. (**1998**). ''Observations of internal solitary waves near the Oregon coast with an inverted echo-sounder,'' J. Geophys. Res. **103(C4)**, 7671–7680.
Vagle, S., Foote, K., Trevorrow, M., and Farmer, D. (**1996**). ''Absolute calibrations of monostatic echosounder systems for bubble counting,'' IEEE J. Ocean. Eng. **21(3)**, 298–305.
Warren, J., Stanton, T., Benfield, M., Wiebe, P., Chu, D., and Sutor, M. (**2001**). ''*In situ* measurements of acoustic target strengths of gas-bearing siphonophores,'' ICES J. Mar. Sci. **58**, 740–749.
Watkins, J., and Brierley, A. (**1996**). ''A post-processing technique to remove background noise from echo integration data,'' ICES J. Mar. Sci. **53**, 339–344.
Wiebe, P., Greene, C., Stanton, T., and Burczynski, J. (**1990**). ''Sound scattering by live zooplankton and micronekton: Empirical studies with a dual beam acoustic system,'' J. Acoust. Soc. Am. **88(5)**, 2346–2360.
Wiebe, P., Stanton, T., Benfield, M., Mountain, D., and Greene, C. (**1997**). ''High-frequency acoustic volume backscattering in the Georges Bank coastal region and its interpretation using scattering models,'' IEEE J. Ocean. Eng. **22(3)**, 445–464.